Control Strategy of a DVR to Improve Stability in Wind Farms Using Squirrel-Cage Induction Generators

Andres E. Leon, *Graduate Student Member, IEEE*, Marcelo F. Farias, Pedro E. Battaiotto, Jorge A. Solsona, *Senior Member, IEEE*, and María Inés Valla, *Fellow, IEEE*

***Abstract*—This work presents a control strategy of a dynamic voltage restorer (DVR) to improve the stability in wind farms based on squirrel-cage induction generators. The DVR controller is tailored to work under unbalanced conditions, which allows overcoming most faults in the power grid. The proposed strategy is capable of balancing voltages at wind farm terminals obtaining several advantages. Firstly, negative-sequence currents are eliminated; thus, overheating, loss of performance, and decreasing of generator useful life are avoided. Secondly, by nullifying negative-sequence voltages, 2ω pulsation in the mechanical torque is prevented, reducing high stress in the turbine mechanical system, especially in the gearbox. The proposed control strategy for the DVR is compatible with farms which already have installed a static VAR compensator. Several scenarios and disturbances, carefully chosen to provide a realistic assessment, have been tested showing the adequacy of the proposed arrangement and controllers.**

***Index Terms*—Dynamic voltage restorer (DVR), fault ride-through capability, grid codes, squirrel-cage induction generators (SCIG), unbalanced conditions, wind energy conversion system (WECS).**

I. Introduction

EVER-INCREASING power generated by wind farms requires that they should be taken into account in the stability studies of the electric network [1]. With over 150 GW of wind power in the world, this sort of Wind Energy Conversion Systems (WECS) becomes very important in the generation array of power systems, especially in some European countries like Denmark, Spain, and Germany, among others. More and more demanding standards are being applied to wind farms in such countries, in order to guarantee stability and power quality of the power systems, even when faults take place in the grid [2]. The main goal of these demanding standards is to avoid disconnection of large wind farms, since a large mismatch between power generation and load consumption may lead to a system collapse.

Currently, new farms are tending to use doubly-fed induction generators (DFIG), or permanent magnet synchronous generators (PMSG) connected to the grid with a back-to-back converter [3]. Nevertheless, over half of the present-day wind farms are still based on squirrel-cage induction generators (SCIG) directly connected to the grid. Solutions based on STATic COMpensators (STATCOMs) are commonly used to allow these wind farms (SCIG-based WECS) to comply with the new demanding standards. This improves the wind farm stability, controlling its reactive power consumption, and regulating the voltage amplitude at the point of common coupling (PCC). However, the power rating of STATCOM should be large, since after a severe fault occurrence, an SCIG can reach reactive power consumption up to twice its rated power.

On the other hand, when the grid provides unbalanced voltages to an SCIG-based WECS, several drawbacks appear. Firstly, due to the low negative-sequence impedance of an SCIG, high currents of negative sequence flow in the stator. These currents produce overheating, loss of performance, and decreasing the generator useful life. Secondly, the interaction of negative-sequence voltages with positive-sequence currents produces a 2ω pulsation in the mechanical torque, which generates a high stress in the turbine mechanical system, especially in the gearbox [4]. These electrical and mechanical problems can activate SCIG protections and disconnect the wind farm. It is worth noting that STATCOMs, operating like a current source, cannot compensate unbalanced voltages arising at the PCC. Since SCIG-based WECSs are very sensitive to this voltage distortion, this issue should be treated differently. Different solutions using STATCOMs [5]–[7], dynamic voltage restorers (DVRs) [8], or back-to-back converters connected to the grid [9], [10] are found in the literature to improve SCIG-based WECS performance. Nevertheless, none of the above-mentioned strategies present a solution or analyze the behavior of the controller when asymmetrical faults or unbalanced voltages arise at the connection point of the wind farm. For this reason, the controlled DVR proposed in this paper is aimed to improve performance of existing wind farms using SCIGs.

Manuscript received May 14, 2010; revised May 18, 2010, September 03, 2010; accepted October 11, 2010. Date of publication November 22, 2010; date of current version July 22, 2011. This work was supported by Universidad Nacional del Sur, Universidad Nacional de La Plata, CONICET, and ANPCyT, Argentina. Paper no. TPWRS-00372-2010.

A. E. Leon and J. A. Solsona are with Instituto de Investigaciones en Ingeniería Eléctrica (IIIE) "Alfredo Desages" (UNS-CONICET), Departamento de Ingeniería Eléctrica y de Computadoras, Universidad Nacional del Sur (UNS), 8000 Bahía Blanca, Argentina (e-mail: aleon@ymail.com; jsolsona@uns.edu.ar).

M. F. Farias and P. E. Battaiotto are with the Laboratorio de Electrónica Industrial, Control e Instrumentación (LEICI), Departamento de Electrotecnia, Facultad de Ingeniería, Universidad Nacional de La Plata (UNLP), 1900 La Plata, Argentina (e-mail: pedro@ing.unlp.edu.ar; marcelo.farias@yahoo.com).

M. I. Valla is with the Laboratorio de Electrónica Industrial, Control e Instrumentación (LEICI), Departamento de Electrotecnia, Facultad de Ingeniería, Universidad Nacional de La Plata (UNLP), 1900 La Plata, Argentina, and also with CONICET, Buenos Aires, Argentina (e-mail: m.i.valla@ieee.org).

Digital Object Identifier 10.1109/TPWRS.2010.2088141

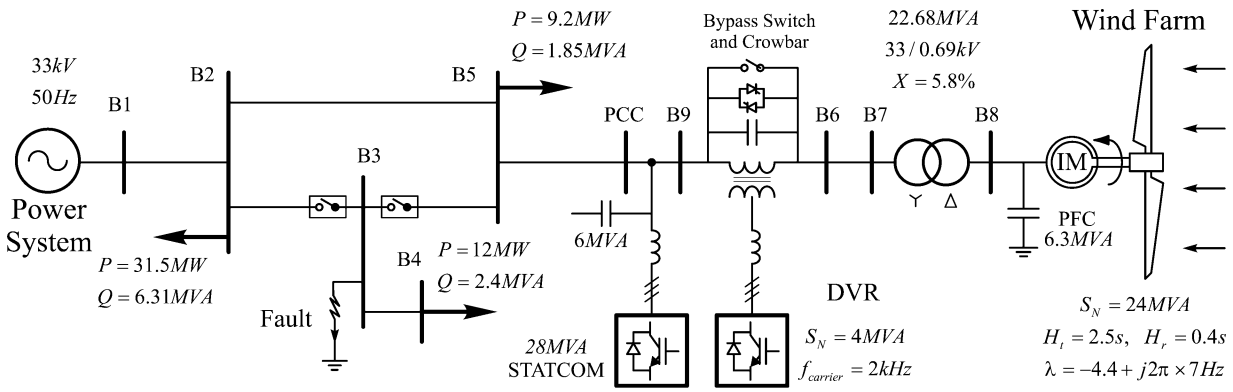

Fig. 1. Power system plus wind farm configurations and parameters used in the tests.

In the case of wind farms using variable speed generators, several strategies to overcome the above-mentioned drawbacks were presented in [11]–[14]. The converters of wind farms based on DFIGs and PMSGs are used to compensate an unbalanced grid voltage. Alternative solutions to eliminate negative-sequence currents in WECSs by using series connected converters can be found in recent references (see [15]–[19]). In [15]–[17], the authors modify the DFIG back-to-back converter topology by connecting the grid-side converter in series with the grid. In this way, the unbalanced grid voltage is compensated by injecting a negative-sequence voltage in series with the DFIG stator. However, in [15], the proposed strategy needs three single-phase converters instead of using a standard three-phase converter, requiring twice the amount of switching devices. In [16] and [17], the control strategies are only focused on the DFIG case, and WECSs based on SCIG are not considered. In [18] and [19], an additional third converter is added, in a series connection, to compensate unbalanced grid voltages.

In this work, a control scheme using a DVR capable of improving the performance and stability of a fixed-speed SCIG-based WECS is proposed. A classical wind farm with a STATCOM for fulfilling reactive power requirements is considered. Since most faults, occurring in distribution systems, are asymmetrical (e.g., single-phase to ground faults), the proposed control strategy is designed in order to control the negative-sequence voltage added in series by the DVR. This allows to compensate unbalanced voltages at the wind farm terminals [20].

The paper is organized as follows: Section II presents the power system, wind farm, and DVR models. The proposed operation philosophy and control strategy are described in Sections III and IV. Performance tests, discussions, and results are shown in Section V. Finally, conclusions are given in Section VI.

II. Power System and DVR Model

A. Power System

The power system under study, including the wind farm, is shown in Fig. 1. The topology and parameters of the system are taken from [5]. The wind farm has 36×600 kW fixed-speed squirrel-cage induction generators, each one with its step-up transformer and power factor correction (PFC) capacitor fixed banks, directly connected to the grid. The considered mechanical subsystem of the WECS consists of two lumped masses (the wind turbine and the electric rotor) connected through a nonrigid shaft. This model presents a gearbox ratio $N_{\rm gb} = 50$, a number of pair of poles $N_r = 2$, and a turbine nominal speed $\omega_{tN} = 30$ RPM.

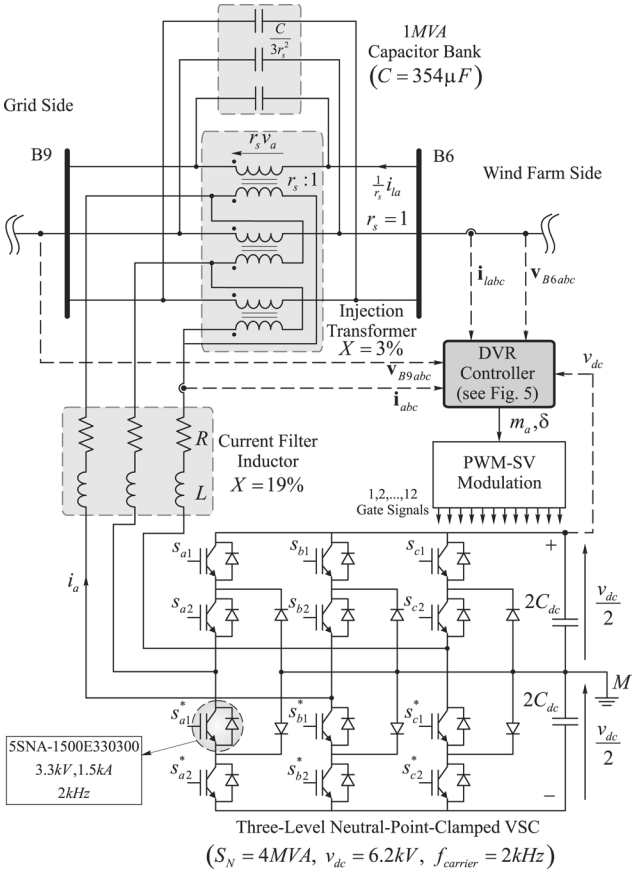

Fig. 2. Electric circuit of the converter and filters used in the DVR implementation.

The proposed DVR is built with a three-level neutral-point-clamped voltage-source converter, and it is placed between the wind farm terminals and the power network. A detailed electric circuit of the converter and filters used in the DVR is shown in Fig. 2.

B. Mathematical Model of the DVR

In order to build the control strategy, it is necessary to obtain a dynamic model of the DVR. Applying the Kirchhoff law to the circuit in Fig. 2, and choosing as state variables: the currents in the inductances $L(i_a, i_b, i_c)$; the voltages of capacitors $C(v_a, v_b, v_c)$; and the dc-bus voltage $(v_{\rm dc})$, it is possible to write the following DVR dynamic model in the α-β stationary reference frame [21]

$$L\dot{i}_\alpha = -Ri_\alpha + e_\alpha - v_\alpha \tag{1}$$
$$L\dot{i}_\beta = -Ri_\beta + e_\beta - v_\beta \tag{2}$$
$$C\dot{v}_\alpha = i_\alpha - i_{l\alpha} \tag{3}$$
$$C\dot{v}_\beta = i_\beta - i_{l\beta} \tag{4}$$
$$C_{\rm dc}\dot{v}_{\rm dc} = -\frac{3}{2}\left(\eta_\alpha i_\alpha + \eta_\beta i_\beta\right) - \frac{v_{\rm dc}}{R_{\rm Loss}} \tag{5}$$

where $i_{l\alpha}$, $i_{l\beta}$ are the wind farm currents in the α-β reference frame. Parameters R, L and C stand for resistance, inductance, and capacitance of DVR input filter, $C_{\rm dc}$ is the capacitance in the dc-bus, $R_{\rm Loss}$ represents the equivalent converter losses, and e_α and e_β are the DVR internal voltages.

The subsystem given by (1)–(4) represents a linear system. Therefore, assuming identical parameters for each phase, the superposition theorem can be applied in order to obtain a converter model for each sequence component (positive and negative), as it is accomplished below.

First, two transformations are defined. One of them $\mathbf{A}(\theta)$ determines a rotating frame in the same direction as the positive-sequence component vector. The other transformation $\mathbf{A}(-\theta)$ determines a rotating frame also at the network frequency, but in opposite direction. Therefore, in a generic vector $\mathbf{x}_{\alpha\beta}$, the positive and negative sequences can be identified [20], [22]. Then, each of them can be transformed to the corresponding reference frame

$$\mathbf{x}_{dq}^{+} = \mathbf{A}(\theta)\mathbf{x}_{\alpha\beta}^{+} \tag{6}$$
$$\mathbf{x}_{dq}^{-} = \mathbf{A}(-\theta)\mathbf{x}_{\alpha\beta}^{-} \tag{7}$$

where $\theta = \omega_s t$ and

$$\mathbf{A}(\theta) = \begin{bmatrix} \cos\theta & -\sin\theta \\ \sin\theta & \cos\theta \end{bmatrix}. \tag{8}$$

These transformations define two d-q reference frames. The first one d-q^+ presents the advantage that rotating components of positive sequence are seen as constant signals, while, in the d-q^- reference frame, the negative-sequence components are also described by constant signals. Then, applying the transformations (6) and (7) to the DVR model (1)–(4), in the α-β^+ and α-β^- stationary reference frames, yields for the d-q^+ reference frame

$$L\dot{i}_d^{+} = -L\omega i_q^{+} + e_d^{+} - v_d^{+} \tag{9}$$
$$L\dot{i}_q^{+} = L\omega i_d^{+} + e_q^{+} - v_q^{+} \tag{10}$$
$$C\dot{v}_d^{+} = -C\omega v_q^{+} + i_d^{+} - i_{ld}^{+} \tag{11}$$
$$C\dot{v}_q^{+} = C\omega v_d^{+} + i_q^{+} - i_{lq}^{+} \tag{12}$$

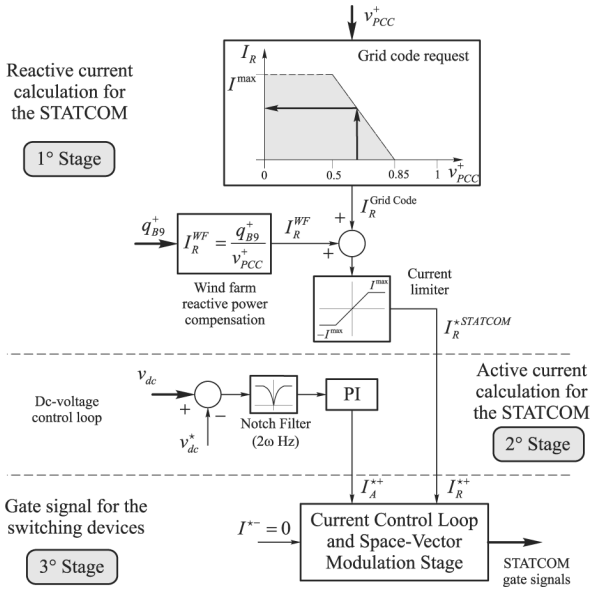

Fig. 3. Simplified scheme of the STATCOM control.

and for the d-q^- reference frame

$$L\dot{i}_d^{-} = L\omega i_q^{-} + e_d^{-} - v_d^{-} \tag{13}$$
$$L\dot{i}_q^{-} = -L\omega i_d^{-} + e_q^{-} - v_q^{-} \tag{14}$$
$$C\dot{v}_d^{-} = C\omega v_q^{-} + i_d^{-} - i_{ld}^{-} \tag{15}$$
$$C\dot{v}_q^{-} = -C\omega v_d^{-} + i_q^{-} - i_{lq}^{-}. \tag{16}$$

The resistance in the power filter inductor was neglected since it verifies that $R \ll \omega L$. The above equations are going to be used in the next sections in order to develop the control strategy to overcome unbalanced conditions.

III. Proposed Operation Philosophy

It is important to assign tasks to be independently accomplished by both the STATCOM and the DVR. To this end, STATCOM current and DVR voltage references should be calculated in a coherent manner. The STATCOM has the standard task of achieving a unity power factor condition and fulfilling the grid code reactive power requirements. The main task of the DVR is eliminating the negative-sequence voltage at the generator terminals, avoiding the above-mentioned drawbacks in the electric machine. Control strategies of both converters are summarized in the following lines.

A. Standard STATCOM Operation Philosophy

The STATCOM main task is to compensate the reactive power consumption of the wind farm. Besides, the STATCOM should fulfill the grid code requirements which demand certain amount of reactive power injection to the grid, in order to support a faulty network [23]. In addition, the dc-bus voltage regulation, as well as a null negative-sequence current injection, must be accomplished.

Based on the above considerations, a control strategy to determine the current references to be injected by the STATCOM

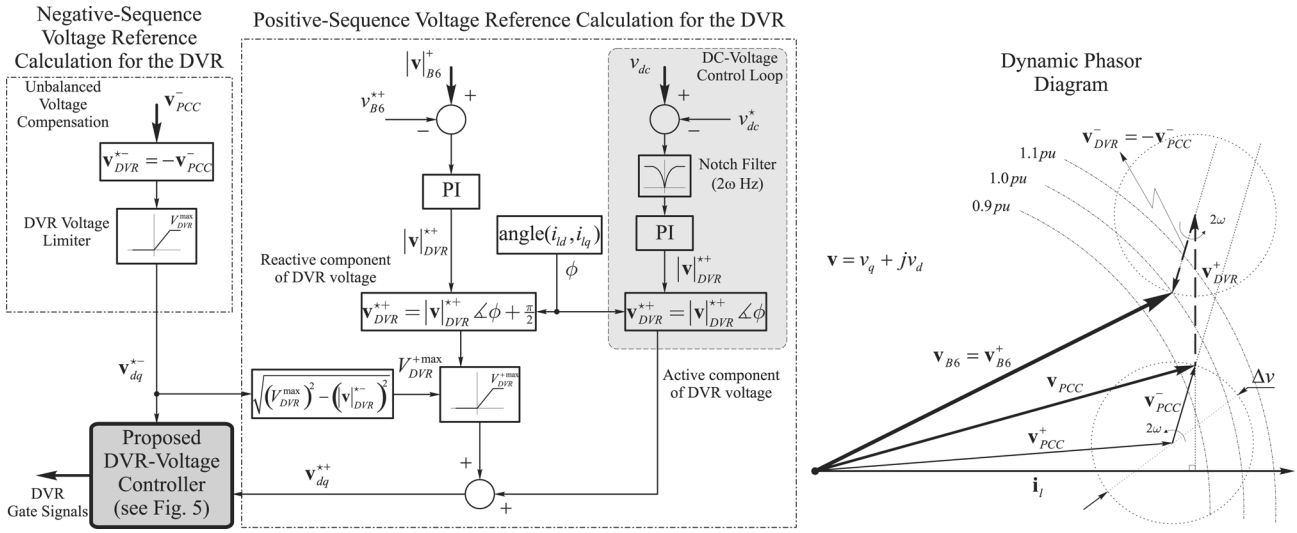

Fig. 4. Simplified scheme for the DVR voltage reference calculation and dynamic phasor diagram in a positive-sequence reference frame.

is shown in Fig. 3. In the first stage, the reactive current component $(I_R^{\text{Grid Code}})$ is obtained by using the grid code requested curve. This fixes the reactive current to be injected according to the PCC voltage level (extracted from [23]). Then, the reactive current absorbed by the wind farm (I_R^{WF}) is also added. The reference current is limited to protect the power switches. In the second stage, the dc-bus voltage is regulated with a PI controller acting on the active current component $(I_A^{\star+})$ to compensate the STATCOM internal losses. Finally, the third stage implements the current control loop to track the current references and the space-vector modulation in order to obtain the STATCOM gate signals. Different current control techniques for the STATCOM can be found in [24]–[26].

B. Proposed DVR Operation Philosophy

The fault level that should be overcome, and the amount of unbalanced voltage which needs to be compensated, determine the power rating required to the DVR. However, economical reasons limit the DVR rated power [27]. In this study, a DVR with a 4-MVA converter plus a 1-MVA capacitor filter is used in a 24-MVA wind farm. Besides, the injected DVR voltage is orthogonal to the line current. In this way, there is no need of a power supply on the dc side.

In Fig. 4, a strategy to define the best utilization of the DVR capacity is presented. When an asymmetric fault takes place, the DVR control gives priority to the negative-sequence voltage compensation. Therefore, the negative-sequence voltage reference for the DVR is $\mathbf{v}_{\text{DVR}}^{\star-} = -\mathbf{v}_{\text{PCC}}^{-}$. Consequently, both the over-current produced by negative-sequence voltages and the mechanical stress due to the 2ω torque pulsations are completely eliminated.

If the negative-sequence voltage compensation action requires less than the rated voltage of the DVR $(|\mathbf{v}|_{\text{DVR}}^{\star-} < V_{\text{DVR}}^{\max})$, then this surplus is used to compensate the positive-sequence voltage component; see sub-block Positive-Sequence Voltage Reference Calculation for the DVR in Fig. 4. This sub-block presents two voltage components. One of them, used for regulating the B6-bus amplitude, is orthogonal to the line current. This avoids the need of a big energy storage system. The second voltage component, used for regulating the dc-voltage, is in phase with the line current. This last component is small since it should only compensate the DVR internal losses. If the fault is not very severe, both compensations may be simultaneously accomplished. For example, the phasor diagram in Fig. 4 shows a PCC-bus voltage composed by a positive- and negative-sequence voltages, $\mathbf{v}_{\text{PCC}} = \mathbf{v}_{\text{PCC}}^{+} + \mathbf{v}_{\text{PCC}}^{-}$. If the DVR performs a full negative-sequence compensation, then its negative-sequence voltage is $\mathbf{v}_{\text{DVR}}^{-} = -\mathbf{v}_{\text{PCC}}^{-}$. Moreover, the PCC-bus positive-sequence voltage, $\mathbf{v}_{\text{PCC}}^{+}$, is lower than 0.9 pu, as can be observed in the phasor diagram. Then, to increase the positive-sequence voltage at the wind farm side, some positive-sequence voltage is added by the DVR, fulfilling $\mathbf{v}_{\text{DVR}}^{+} \perp \mathbf{i}_l$. Consequently, the B6-bus voltage results being negative-sequence-free and within the allowed boundaries of positive-sequence voltages, $\mathbf{v}_{B6} = \mathbf{v}_{B6}^{+} = \mathbf{v}_{\text{PCC}} + \mathbf{v}_{\text{DVR}}$.

The technique described in [22] is used here to separate the sequence components of the voltage and current signals needed for the implementation of the control law.

IV. DVR Converter Control Strategy

In this section, a control law to generate the PWM space vector of the DVR converter is presented. This law allows to follow the previously calculated positive $\mathbf{v}_{dq}^{\star+}$ and negative $\mathbf{v}_{dq}^{\star-}$ sequence voltage references (see Fig. 4).

The DVR dynamic model (9)–(16), obtained in Section II, can be split in two subsystems. The first one (9)–(12) is in the d-q^{+} reference frame, while the second one (13)–(16) is in the d-q^{-} reference frame. As both subsystems are now decoupled, independent control strategies can be designed for both sequence components. The controllers can be easily tuned, since in each d-q reference frame, the signals to be controlled are constant.

The capacitor filter voltages, v_d and v_q, are the states to be controlled. These voltages are going to be applied in series at the wind farm terminals. However, it can be seen that the dynamic model (9)–(12) constitutes a coupled system. Moreover, the control inputs (e_d, e_q) are not directly associated to the

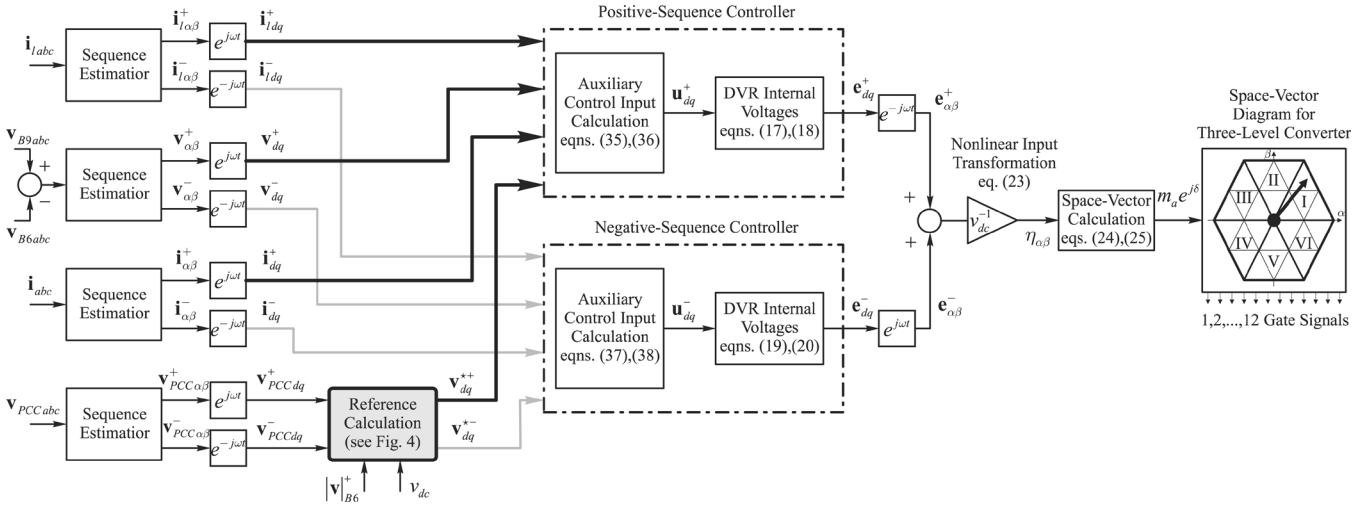

Fig. 5. Block diagram of the proposed DVR control strategy.

filter voltage dynamics (voltage relative degree equal to two). In order to overcome this problem, cascade controls were used in [28]–[30]. However, this technique presents the drawback that the outer voltage loop should be slow to avoid interaction with the cascade inner current loop. Therefore, a procedure based on feedback linearization is accomplished to obtain a control law that directly manipulates the capacitor voltage, in a decoupled manner. So, DVR internal voltages e_d^+, e_q^+, e_d^-, and e_q^- are calculated from (17)–(20) (details of the control law derivation are provided in the Appendix):

$$e_d^+ = L(C(u_d^+ + \omega^2 v_d^+) + 2\omega i_q^+ - \omega i_{lq}^+) + v_d^+ \quad (17)$$

$$e_q^+ = L(C(u_q^+ + \omega^2 v_q^+) - 2\omega i_d^+ + \omega i_{ld}^+) + v_q^+ \quad (18)$$

$$e_d^- = L(C(u_d^- + \omega^2 v_d^-) - 2\omega i_q^- + \omega i_{lq}^-) + v_d^- \quad (19)$$

$$e_q^- = L(C(u_q^- + \omega^2 v_q^-) + 2\omega i_d^- - \omega i_{ld}^-) + v_q^-. \quad (20)$$

The actual control inputs which drive the DVR voltage-source converter are the signals η_α and η_β, which are related with the DVR internal voltages by

$$e_\alpha \triangleq \eta_\alpha v_{\rm dc} \quad (21)$$

$$e_\beta \triangleq \eta_\beta v_{\rm dc}. \quad (22)$$

Then, the control inputs η_α and η_β are obtained from (6) and (7), and using (21) and (22), resulting

$$\begin{bmatrix}\eta_\alpha \\ \eta_\beta\end{bmatrix} = \frac{1}{v_{\rm dc}}\left(\mathbf{A}^{-1}(\theta)\begin{bmatrix}e_d^+ \\ e_q^+\end{bmatrix} + \mathbf{A}^{-1}(-\theta)\begin{bmatrix}e_d^- \\ e_q^-\end{bmatrix}\right). \quad (23)$$

The amplitude and phase needed for the space-vector modulation (SVM) stage are calculated as

$$m_a = \sqrt{\eta_\alpha^2 + \eta_\beta^2} \quad (24)$$

$$\delta = \arctan(\eta_\alpha, \eta_\beta). \quad (25)$$

The control law (23) is nonlinear because it has the state $v_{\rm dc}$ in the denominator. This allows compensating the dc-bus voltage variation and to avoid low order harmonics in the DVR currents and voltages. These harmonics appear when a dc-bus voltage ripple with a frequency of 2ω exists due to unbalanced grid conditions. A block diagram of the whole DVR converter control strategy is shown in Fig. 5.

V. Performance Testing

The proposed strategy was evaluated through several tests. In this section, the most relevant results are presented. The power system, DVR converter, and controller were implemented in the SimPowerSystems blockset of SIMULINK/MATLAB®. The power system configuration and parameters used in these tests are shown in Fig. 1.

A. Unbalanced Voltage Compensation

The first test considers a 500-ms single-phase-to-ground fault through impedance in the B3 bus (see Fig. 1). Fig. 6 shows currents and voltages immediately after the fault occurs. Fig. 6(a) illustrates the PCC voltage waveforms. The voltage unbalance during the fault is clearly observed. On the other hand, Fig. 6(b) shows that the terminal voltages of the wind farm (B8 bus) are perfectly balanced. Consequently, the currents in the SCIG stator are also balanced—see Fig. 6(c). Fig. 6(d) shows the voltages injected by the DVR.

Negative-sequence voltages in both PCC and B8 buses are depicted in Fig. 7(a). It is observed that the negative-sequence voltage component which appears in the PCC bus, due to the asymmetrical fault, is quickly nullified at the wind farm side (B8 bus) by the DVR compensation. Fig. 7(b)–(e) illustrates the electromagnetic torque and mechanical speed of the SCIG with and without the proposed DVR compensation. A high 2ω pulsation in the generator torque is observed when the proposed compensation is not implemented. This oscillation is around $\pm 40\%$ of the nominal torque during the fault period—see zoom in Fig. 7(b). When the proposed DVR-based compensation is applied, this 2ω pulsation is nullified, as it can be seen in Fig. 7(c). In this way, the SCIG electromagnetic torque is maintained almost constant during the whole fault period. Fig. 7(d) and (e) shows the rotor (thick line) and turbine (thin line)

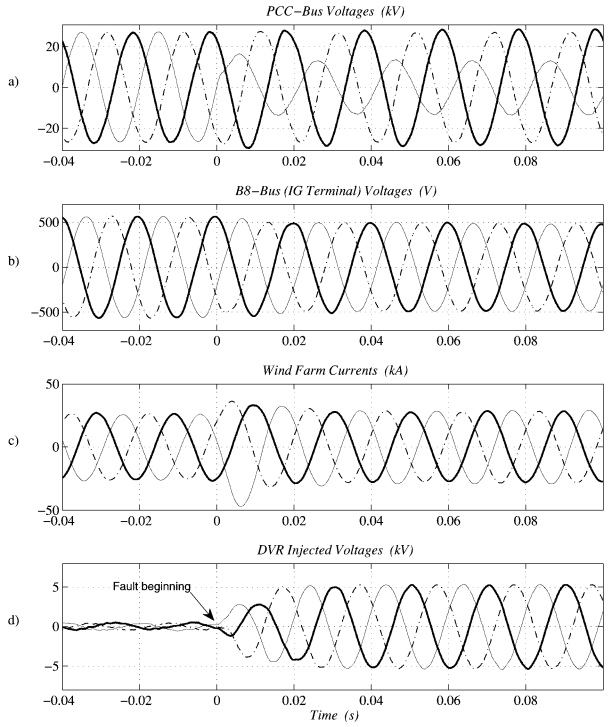

Fig. 6. Current and voltage waveforms after the asymmetrical fault.

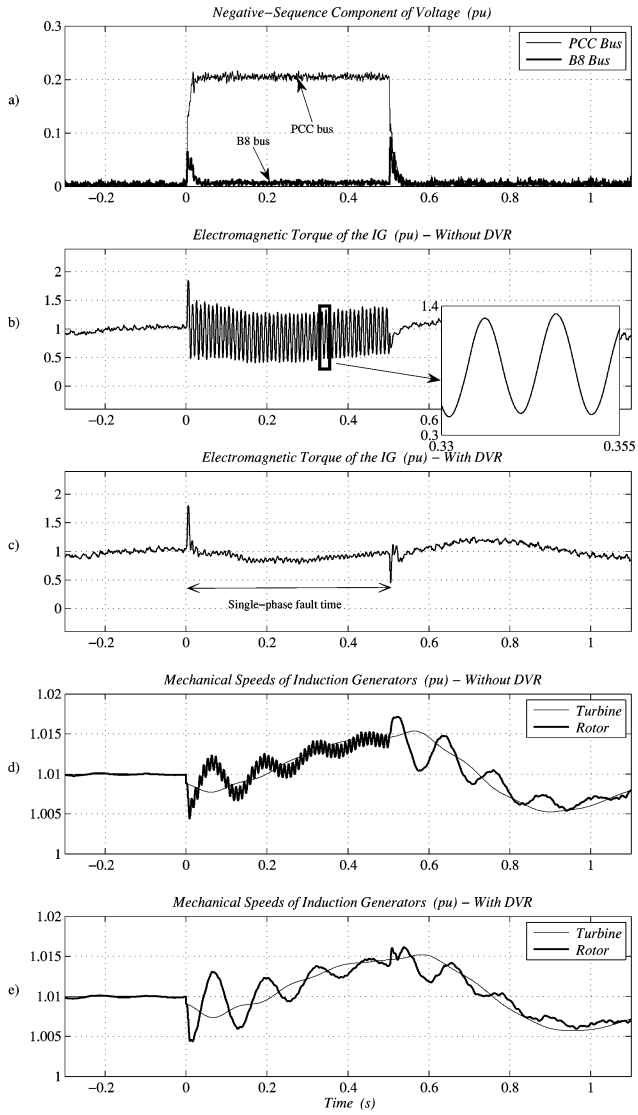

Fig. 7. Compensation of unwanted effects in the SCIG due to unbalanced conditions.

speeds. Fig. 7(d) shows that the 2ω oscillation also appears in the rotor speed when the DVR is not used. Fig. 7(e) shows that the 2ω oscillation has been completely eliminated by the DVR action. This makes possible to reduce the mechanical efforts over the whole gear train of the wind generator.

B. Stability Enhancement Against Faults

The original wind farm was designed with a STATCOM power in order to fulfill short circuits up to 500 ms, such as demanded by the Spanish standard [23]. Now, it is studied how the addition of a DVR, with only a fraction of the farm power, along with the proposed control strategy can reach more demanding grid operation codes, for example to ride-through short circuits of 650 ms. Therefore, 500-ms and a 650-ms three-phase fault in B3 bus are evaluated with different tests. The results are presented in Figs. 8 and 9, respectively.

The PCC-bus voltage amplitude and the turbine speed are depicted in subplots a) and b). Subplots c) and d) show the reactive power at the B8 and PCC buses, for the cases with and without the proposed DVR compensation. The gray area represents a capacitive reactive power (injected from the farm to the grid), while the black area indicates an inductive reactive power (absorb by the farm from the grid). As it is expected for a 500-ms fault, both solutions, with only STATCOM and with the STATCOM plus the DVR, can fulfill the reactive power requirements and stabilize the wind farm (see Fig. 8). However, for a 650-ms short circuit, the case with only STATCOM cannot fulfill the grid code requirements and stabilize the farm properly. Namely, the PCC-bus voltage after the fault is out of the $\pm 10\%$ boundaries—see Fig. 9(a). The SCIG slip increases up to 8% and decreases very slowly, so that 150 ms after the fault is finished, the wind farm is still consuming inductive reactive power from the grid, which is not allowed by wind farm grid codes—see Fig. 9(c). On the other hand, all this drawbacks disappear when the proposed DVR-based strategy is used, as can be observed in Fig. 9. Thus, the proposed scheme, besides the above-mentioned benefits under unbalanced conditions, also allows to ride through more demanding balanced short circuits.

C. Internal Fault Assessment

This last test is carried out in order to verify both the ride-through capability and reliable implementation of the proposed DVR strategy against an internal fault. A severe three-phase fault is performed at the B6 bus, isolating the two converters from the generator (see Fig. 1). Fig. 10(a) illustrates the depth of voltage sag at the PCC and B6 buses. Machine acceleration, during the fault time, can be seen in rotor and turbine speeds in Fig. 10(b). Fig. 10(c) depicts the reactive power at the PCC and B6 buses. Clearly, the wind farm can fulfill the grid code requirements regarding reactive power consumption at the PCC bus, even with a severe internal fault in the wind farm. Fig. 10(d)

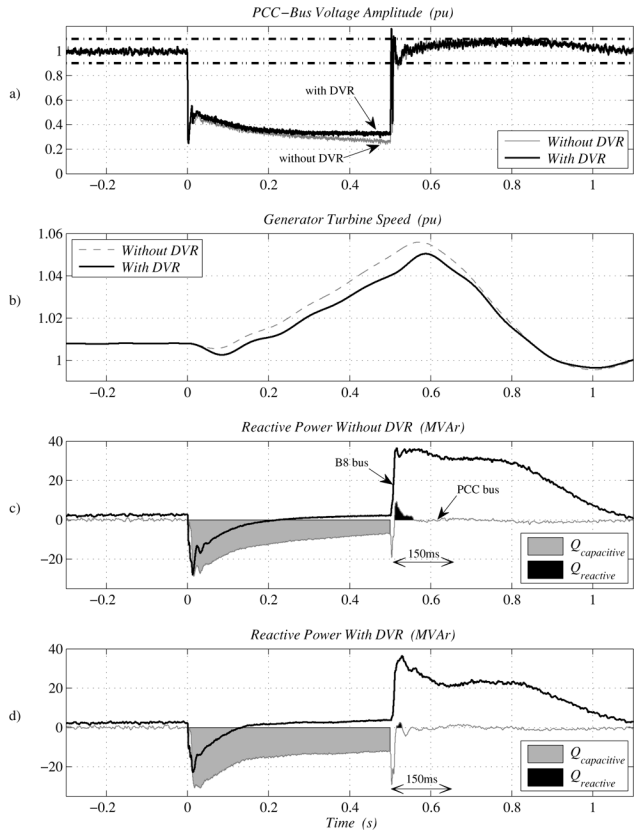

Fig. 8. System response against a 500-ms three-phase fault with and without the proposed DVR compensation.

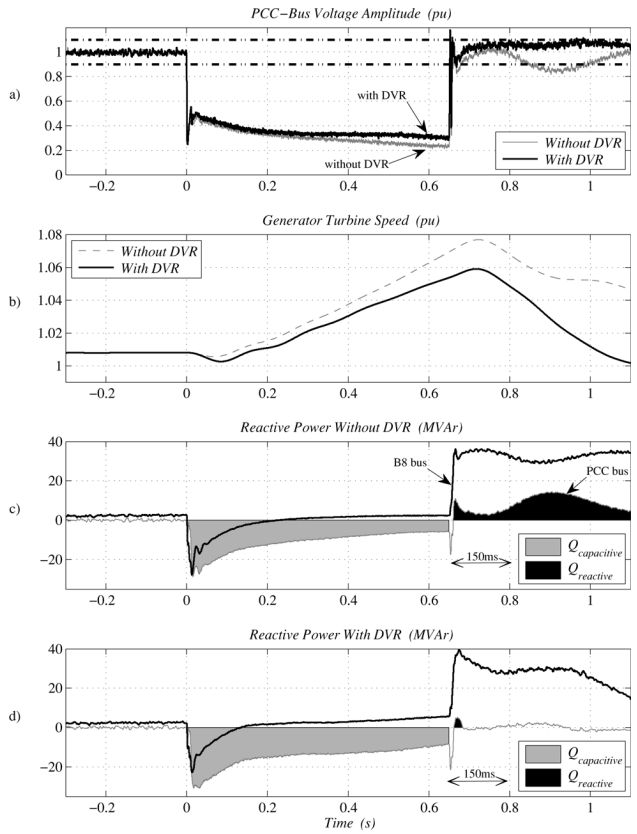

Fig. 9. System response against a 650-ms three-phase fault with and without the proposed DVR compensation.

shows that the dc-bus voltage in the DVR converter is perfectly regulated before, during, and after the internal fault.

VI. Conclusion

In this work, an alternative proposal for improving SCIG-based WECSs is presented. Different to classical solution, where only a STATCOM is used, the main idea is to combine a STATCOM with a DVR converter managing their tasks so that they can independently work in a proper way. The proposed DVR control strategy is tailored in order to work under unbalanced conditions, allowing to overcome most faults in the power grid. As a summary of the proposed strategy advantages it can be said that, under balanced conditions: 1) the grid-code reactive power requirements are fulfilled, 2) the low voltage ride-through capability is enhanced and it can support short circuits of larger duration, which goes in concordance with more and more demanding standards. On the other hand, under unbalanced conditions: 1) voltages at the wind farm terminals are balanced when asymmetrical faults occur in the power network; 2) the negative-sequence currents in the SCIG are eliminated, avoiding overheating, loss of performance, and decreasing of generator useful life; 3) the 2ω pulsation in the mechanical torque is prevented, reducing high stress in the turbine mechanical system, especially in the gearbox. In this way, the danger of disconnection of the wind farm, due to activation of the SCIG protections, is reduced.

In wind farms which already have STATCOMs with the aim of fulfilling the current demanding standards, the proposed

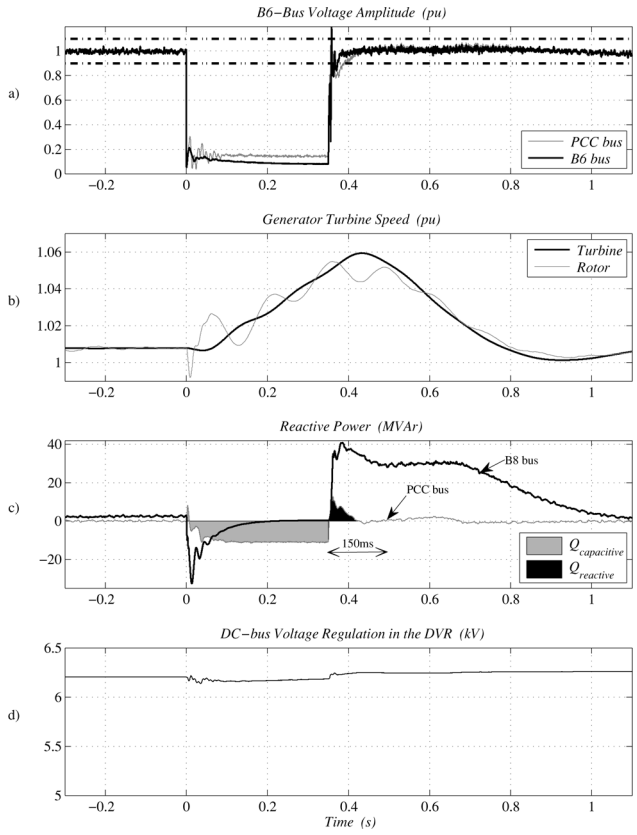

Fig. 10. DVR plus wind farm behavior against an internal fault at the B6 bus.

solution to include a small DVR allows enhancing the stability margin. Additionally, the DVR will allow isolating the wind farm from the negative-sequence voltage components which arise under unbalanced conditions in the electric network. A different situation arises in wind farms where the inclusion of a STATCOM is being projected. In these cases, the proposed DVR inclusion will allow fulfilling the same requirements of fault ride-through demanded by the standards, but using a STATCOM with a smaller rated power. At the same time, due to the characteristic of the DVR of eliminating negative-sequence voltage components, a better performance of the wind farm under unbalanced conditions is also obtained. Several tests have been assessed showing that the proposed DVR control strategy is an attractive choice to maintain working the present wind farms, in spite of ever-increasing grid code requirements.

APPENDIX

The development and derivation of the control law in order to manipulate the DVR injected voltages will be accomplished in this Appendix. Firstly, the states v_d^+, v_q^+, v_d^-, and v_q^-, from (9)–(16), are twice differentiated with respect to time

$$\ddot{v}_d^+ = \frac{1}{C}\left(\frac{e_d^+ - v_d^+}{L} - 2\omega i_q^+ + \omega i_{lq}^+\right) - \omega^2 v_d^+ \triangleq u_d^+ \quad (26)$$

$$\ddot{v}_q^+ = \frac{1}{C}\left(\frac{e_q^+ - v_q^+}{L} + 2\omega i_d^+ - \omega i_{ld}^+\right) - \omega^2 v_q^+ \triangleq u_q^+ \quad (27)$$

$$\ddot{v}_d^- = \frac{1}{C}\left(\frac{e_d^- - v_d^-}{L} + 2\omega i_q^- - \omega i_{lq}^-\right) - \omega^2 v_d^- \triangleq u_d^- \quad (28)$$

$$\ddot{v}_q^- = \frac{1}{C}\left(\frac{e_q^- - v_q^-}{L} - 2\omega i_d^- + \omega i_{ld}^-\right) - \omega^2 v_q^- \triangleq u_q^-. \quad (29)$$

Previous equations (26)–(29) have allowed defining the auxiliary control inputs u_d^+, u_q^+, u_d^-, and u_q^-. These auxiliary inputs are going to be used in order to accomplish a direct and decoupled control over the DVR injected voltage. From (26)–(29), the internal voltages of the DVR converter e_d^+, e_q^+, e_d^-, and e_q^-, see (17)–(20), are obtained.

Therefore, by using the input transformations (17)–(20), the transform system has a linear and decoupled form, see (30)–(33), whose states not only are constant but also are directly the states of interest in order to achieve the desired compensation over the wind farm:

$$\ddot{v}_d^+ = u_d^+ \quad (30)$$

$$\ddot{v}_q^+ = u_q^+ \quad (31)$$

$$\ddot{v}_d^- = u_d^- \quad (32)$$

$$\ddot{v}_q^- = u_q^-. \quad (33)$$

Note that the systems (30)–(33) have a structure of the general form $\ddot{v} = u$. Since the relative degree of v is two, a second-order tracking error dynamics is chosen as $\ddot{\tilde{v}} + k_1\dot{\tilde{v}} + k_2\tilde{v} = 0$, where the tracking error is defined as $\tilde{v} \triangleq v - v^\star$. From this last equation, the auxiliary control input, u, can be obtained

$$u = -k_1\dot{v} - k_2\left(v - v^\star\right) \quad (34)$$

the superscript "$\star$" denotes desired reference value, and k_1 and k_2 gains are design coefficients which define the tracking error dynamics. Then, the four auxiliary control inputs u_d^+, u_q^+, u_d^-, and u_q^- can be obtained from the general expression (34), resulting

$$u_d^+ = -k_1\left(-\omega v_q^+ + \frac{1}{C}(i_d^+ - i_{ld}^+)\right) - k_2(v_d^+ - v_d^{\star+}) \quad (35)$$

$$u_q^+ = -k_1\left(\omega v_d^+ + \frac{1}{C}(i_q^+ - i_{lq}^+)\right) - k_2(v_q^+ - v_q^{\star+}) \quad (36)$$

$$u_d^- = -k_1\left(\omega v_q^- + \frac{1}{C}(i_d^- - i_{ld}^-)\right) - k_2(v_d^- - v_d^{\star-}) \quad (37)$$

$$u_q^- = -k_1\left(-\omega v_d^- + \frac{1}{C}(i_q^- - i_{lq}^-)\right) - k_2(v_q^- - v_q^{\star-}) \quad (38)$$

where expressions (11), (12), (15), and (16) were used. The last equations represent the auxiliary control inputs required to calculate the DVR internal voltages of (17)–(20).

REFERENCES

[1] E. Vittal, M. O'Malley, and A. Keane, "A steady-state voltage stability analysis of power systems with high penetrations of wind," *IEEE Trans. Power Syst.*, vol. 25, no. 1, pp. 433–442, Feb. 2010.

[2] S. Muyeen, R. Takahashi, T. Murata, and J. Tamura, "A variable speed wind turbine control strategy to meet wind farm grid code requirements," *IEEE Trans. Power Syst.*, vol. 25, no. 1, pp. 331–340, Feb. 2010.

[3] J. M. Carrasco, L. G. Franquelo, J. T. Bialasiewicz, E. Galvan, R. C. P. Guisado, M. A. M. Prats, J. I. León, and N. Moreno-Alfonso, "Power-electronic systems for the grid integration of renewable energy sources: A survey," *IEEE Trans. Ind. Electron.*, vol. 53, pp. 1002–1016, Jun. 2006.

[4] J. M. Mauricio, A. E. Leon, A. Gomez-Exposito, and J. A. Solsona, "An electrical approach to mechanical effort reduction in wind energy conversion systems," *IEEE Trans. Energy Convers.*, vol. 23, no. 4, pp. 1108–1110, Dec. 2008.

[5] Z. Saad-Saoud, M. L. Lisboa, J. B. Ekanayake, N. Jenkins, and G. Strbac, "Application of STATCOMs to wind farms," *Proc. Inst. Elect. Eng., Gen., Transm., Distrib.*, vol. 145, no. 5, pp. 511–516, Sep. 1998.

[6] I. Tamrakar, L. B. Shilpakar, B. G. Fernandes, and R. Nilsen, "Voltage and frequency control of parallel operated synchronous generator and induction generator with STATCOM in micro hydro scheme," *IET Gen., Transm., Distrib.*, vol. 1, pp. 743–750, Sep. 2007.

[7] H. Gaztanaga, I. Etxeberria-Otadui, D. Ocnasu, and S. Bacha, "Real-time analysis of the transient response improvement of fixed-speed wind farms by using a reduced-scale STATCOM prototype," *IEEE Trans. Power Syst.*, vol. 22, no. 2, pp. 658–666, May 2007.

[8] H. Gaztanaga, I. Etxeberria-Otadui, S. Bacha, and D. Roye, "Fixed-speed wind farm operation improvement by using DVR devices," in *Proc. IEEE Int. Symp. Industr. Electr. (ISIE'07)*, Jun. 2007, pp. 2679–2684.

[9] X. I. Koutiva, T. D. Vrionis, N. A. Vovos, and G. B. Giannakopoulos, "Optimal integration of an offshore wind farm to a weak AC grid," *IEEE Trans. Power Del.*, vol. 21, no. 2, pp. 987–994, Apr. 2006.

[10] W. Lu and B. T. Ooi, "Multiterminal LVDC system for optimal acquisition of power in wind-farm using induction generators," *IEEE Trans. Power Electron.*, vol. 17, pp. 558–563, Jul. 2002.

[11] L. Xu and Y. Wang, "Dynamic modeling and control of DFIG-based wind turbines under unbalanced network conditions," *IEEE Trans. Power Syst.*, vol. 22, no. 1, pp. 314–323, Feb. 2007.

[12] T. K. A. Brekken and N. Mohan, "Control of a doubly fed induction wind generator under unbalanced grid voltage conditions," *IEEE Trans. Energy Convers.*, vol. 22, no. 1, pp. 129–135, Mar. 2007.

[13] C. H. Ng, L. Ran, and J. Bumby, "Unbalanced-grid-fault ride-through control for a wind turbine inverter," *IEEE Trans. Ind. Appl.*, vol. 44, pp. 845–856, May–Jun. 2008.

[14] G. Saccomando, J. Svensson, and A. Sannino, "Improving voltage disturbance rejection for variable-speed wind turbines," *IEEE Trans. Energy Convers.*, vol. 17, no. 3, pp. 422–428, Sep. 2002.

[15] N. Joshi and N. Mohan, "A novel scheme to connect wind turbines to the power grid," *IEEE Trans. Energy Convers.*, vol. 24, no. 2, pp. 504–510, Jun. 2009.
[16] B. Singh, V. Emmoji, S. Singh, and I. Erlich, "Performance evaluation of new series connected grid-side converter of doubly-fed induction generator," in *Proc. Int. Conf. Power System Technology and IEEE Power India Conf. (POWERCON'08)*, Oct. 2008, pp. 1–8.
[17] J. Massing and H. Pinheiro, "Design and control of doubly-fed induction generators with series grid-side converter," in *Proc. 34th Annu. Conf. IEEE Industrial Electronics (IECON'08)*, Nov. 2008, pp. 139–145.
[18] P. Flannery and G. Venkataramanan, "Unbalanced voltage sag ride-through of a doubly fed induction generator wind turbine with series grid-side converter," *IEEE Trans. Ind. Appl.*, vol. 45, pp. 1879–1887, Sep.–Oct. 2009.
[19] B. Singh, V. Emmoji, and S. Singh, "Performance evaluation of series and parallel connected grid side converters of DFIG," in *Proc. IEEE Power and Energy Soc. General Meeting*, Jul. 2008, pp. 1–8.
[20] M. I. Marei, E. F. El-Saadany, and M. M. A. Salama, "A new approach to control DVR based on symmetrical components estimation," *IEEE Trans. Power Del.*, vol. 22, no. 4, pp. 2017–2024, Oct. 2007.
[21] C. Zhan, A. Arulampalam, and N. Jenkins, "Four-wire dynamic voltage restorer based on a three-dimensional voltage space vector pwm algorithm," *IEEE Trans. Power Electron.*, vol. 18, pp. 1093–1102, Jul. 2003.
[22] H.-S. Song, I.-W. Joo, and K. Nam, "Source voltage sensorless estimation scheme for PWM rectifiers under unbalanced conditions," *IEEE Trans. Ind. Electron.*, vol. 50, pp. 1238–1245, Dec. 2003.
[23] Red Eléctrica. P.O. 12.3, "Requisitos de respuesta frente a huecos de tensión de las instalaciones de producción en régimen especial. Spanish regulations (in Spanish)," *Spanish Ministry of Industry, Tourism and Commerce. BOE Núm.* vol. 254, pp. 1–7, Oct. 2006. [Online]. Available: http://www.ree.es.
[24] C. Hochgraf and R. H. Lasseter, "Statcom controls for operation with unbalanced voltages," *IEEE Trans. Power Del.*, vol. 13, no. 2, pp. 538–544, Apr. 1998.
[25] A. Yazdani and R. Iravani, "A unified dynamic model and control for the voltage-sourced converter under unbalanced grid conditions," *IEEE Trans. Power Del.*, vol. 21, no. 3, pp. 1620–1629, Jul. 2006.
[26] A. E. Leon, J. M. Mauricio, J. A. Solsona, and A. Gomez-Exposito, "Software sensor-based STATCOM control under unbalanced conditions," *IEEE Trans. Power Del.*, vol. 24, no. 3, pp. 1623–1632, Jul. 2009.
[27] V. K. Ramachandaramurthy, A. Arulampalam, C. Fitzer, C. Zhan, M. Barnes, and N. Jenkins, "Supervisory control of dynamic voltage restorers," *Proc. Inst. Elect. Eng., Gen., Transm., Distrib.*, vol. 151, no. 4, pp. 509–516, Jul. 2004.
[28] H. Awad, J. Svensson, and M. Bollen, "Mitigation of unbalanced voltage dips using static series compensator," *IEEE Trans. Power Electron.*, vol. 19, pp. 837–846, May 2004.
[29] M. Bongiorno, J. Svensson, and A. Sannino, "An advanced cascade controller for series-connected VSC for voltage dip mitigation," *IEEE Trans. Ind. Appl.*, vol. 44, no. 1, pp. 187–195, Jan.–Feb. 2008.
[30] Y. W. Li, F. Blaabjerg, D. M. Vilathgamuwa, and P. C. Loh, "Design and comparison of high performance stationary-frame controllers for DVR implementation," *IEEE Trans. Power Electron.*, vol. 22, pp. 602–612, Mar. 2007.

Andres E. Leon (S'02–GS'05) was born in Argentina in 1979. He received the electrical engineering degree from the National University of Comahue, Neuquén, Argentina, in 2005. He is currently pursuing the Ph.D. degree in control systems at the Instituto de Investigaciones en Ingeniería Eléctrica "Alfredo Desages" (IIIE), Universidad Nacional del Sur, Bahía Blanca, Argentina.

His primary areas of interest are power systems control, custom power systems, and wind energy conversion systems.

Marcelo F. Farias was born in Villa Gesell, Argentina, on January 17, 1975. He received the Engineer degree from La Plata National University, Buenos Aires, Argentina, in 2006.

He has worked as a researcher for since 2007. Currently, he is an Assistant Professor in the Electrical Engineering Department at Universidad Nacional de La Plata, La Plata, Argentina. His research interests include power electronics, power quality, and power systems operation and control.

Pedro E. Battaiotto received the Electronics Engineer degree from National University of La Plata (UNLP), Buenos Aires, Argentina, in 1977.

Currently, he is a Full Professor in the Electrical Engineering Department at UNLP, where he has been since 1991. He was a Scientific Associate at the European Organization for Nuclear Research (CERN), Switzerland, from 1986 to 1987. He was a Scientific Associate at Microprocessors Lab-INFN-International Center for Theoretical Physics (ICTP), Trieste, Italy, from 1988 to 1989. His primary area of interest is power electronics and control in energy conversion systems.

Jorge A. Solsona (SM'04) received the electronics engineer and Dr. degrees from the Universidad Nacional de La Plata, La Plata, Argentina, in 1986 and 1995, respectively.

Currently, he is with the Instituto de Investigaciones en Ingeniería Eléctrica Alfredo Desages (IIIE), Departamento de Ingeniería Eléctrica y de Computadoras, Universidad Nacional del Sur, Bahía Blanca, Argentina, and CONICET, where he is involved in teaching and research on control theory and its applications to electromechanical systems.

María Inés Valla (S'79–M'80–SM'97–F'10) received the Electronics Engineer and Doctor in Engineering degrees from the National University of La Plata (UNLP), La Plata, Argentina, in 1980 and 1994, respectively.

She is currently a Full Professor in the Electrical Engineering Department, Engineering Faculty, UNLP. She is also with the Consejo Nacional de Investigaciones Científicas y Técnicas, Buenos Aires, Argentina. She is engaged in teaching and research on power converters and ac motor drives.

Dr. Valla is a member of the Buenos Aires Academy of Engineering in Argentina. She is the VP for Membership of the IEEE Industrial Electronics Society.